Proceedings of IMECE2008
2008 ASME International Mechanical Engineering Congress and Exposition
October 31-November 6, 2008, Boston, Massachusetts, USA

IMECE2008-68082

A METHODOLOGY FOR APPLYING ENERGY HARVESTING TO EXTEND WILDLIFE TAG LIFETIME

Robert MacCurdy
Cornell University
Lab of Ornithology
Ithaca, NY, U.S.A.

Timothy Reissman
Cornell University
Mechanical Engineering
Ithaca, NY, U.S.A

Ephrahim Garcia
Cornell University
Aerospace Engineering
Ithaca, NY, U.S.A

David Winkler
Cornell University
Ecology & Evolutionary Biology
Ithaca, NY, U.S.A.

ABSTRACT

Wildlife monitoring tags are a widely used technique for studying animals in their natural habitats. At present, these devices are energy limited, based on the mass of the electrochemical battery that can be carried by the animal. Flying animals are particularly restricted, based on a requirement for minimal excess loading. This requirement causes tag lifetimes to be far shorter than would be useful from an ecological perspective, particularly for smaller animals. Energy harvesting is being widely adopted in applications where access to permanent power is limited. If applied to wildlife tags, this approach offers the possibility of extending functional lifetimes indefinitely; however, it presents unique challenges. Practical applications on flying animals are extremely mass limited, subject to environmental stress, and operate at very low frequencies. This paper is meant to address the critical issues in the design task, and makes attempts to place bounds on unknown design parameters, based on literature research where applicable, and on experiment when no data exists. We discuss candidate harvester materials, novel data acquisition tools, and a prototype harvester design.

INTRODUCTION

Wildlife monitoring and tracking tags enable biologists to gather detailed data on numerous environmental and ecological phenomena. These devices multiply the efforts of biologists and conservationists, allowing them to obtain information, even in real time, that would otherwise be impossible or would require enormous effort to sample. Wildlife tags have been used to sample location, activity, vocalizations, temperature, heart rate, blood flow, muscle activity and many other parameters [1]. Early applications for radio tracking include work by LeMunyan [2] and Cochran [3]. In the nearly sixty years since, wildlife tags have become smaller, and some now include microelectronics for control and data storage. While microelectronics have followed Moore's law toward smaller size, advances in power consumption and battery energy density have not kept pace. Battery lifetime imposes a hard limit on the performance of small tags for animal study. Radio-tracking tags are widely used to monitor animal movements, but the power consumption of these tags limits their use to a year or less. Multi-year lifetimes for tracking tags would enable researchers to observe animal migration patterns over multiple seasons, or track dispersal as animals mature. This information is not attainable with current battery technology. Larger batteries are certainly available, and are appropriate for some species, but for the vast majority of flying animals, larger and heavier batteries are simply not an option. While additional on-board energy storage may not be currently feasible, new developments in the area of energy harvesting provide promising means to extend tag lifetimes.

Multiple sources of ambient energy are available for harvesting, including thermal, solar and vibration, but some are more feasible than others. While the animal's core temperature is often well above the ambient temperature, low coupling coefficients, and the relatively large mass required by an effective heat sink, preclude the thermoelectric generator for very low mass systems. Solar energy is appealing; however measurements have shown that feathers and fur absorb solar energy very well. Even a single feather above a solar cell

causes a dramatic reduction in the power output. While feathers can be trimmed, their re-growth can still limit tag lifetime.

Piezoelectric benders offer the potential for a straightforward means of harvesting available mechanical energy. They can be scaled to the application and provide a convenient voltage output. Integrating the piezoelectric material into the system remains a challenge. Piezoelectric benders can be efficient power absorbers when tuned and driven at resonance; however, there may be significant variability in the driving frequency and amplitude when the piezoelectric device is actually attached to an animal. While many animals have been measured for wing beat frequency, little is known about the acceleration of the body, to which a piezoelectric device would be attached. Environmental considerations and attachment techniques also present challenges to successful integration. The piezoelectric material must be efficiently coupled to the animal's body, yet must not impede normal behavior or interfere with flight. It must be well sealed, and robust enough to tolerate routine manipulation by the animal (preening, etc), as well as small or flexible enough to avoid snagging on branches or roost holes.

The low amount of energy available for harvesting, and its intermittent nature, require a system for accumulation and storage. We are integrating piezoelectric vibration power harvesters with electronics for rectification, storage and power management into tags weighing a few grams. The control strategy chosen impacts the rate of available energy captured and an optimal strategy will maximize energy capture from an intermittent source. We have developed a very simple circuit using a bang-bang controller, as well as one based on a microcontroller, which enables more sophisticated control. The tag stores energy when it is available, and when sufficient energy has been accumulated, the power management system makes it available to other systems in the tag. This approach can extend the tag lifetime indefinitely. One version of the tag employs a light sensor and an RF transceiver to measure sunrise and sunset times, archive them locally and transmit them to a receiving station when within range. This system will allow researchers to monitor wildlife migration patterns automatically via solar geolocation techniques similar to those used by sailors before the advent of modern navigation equipment. Another version of this tag is meant to supply power to a suite of sensors carried by a large moth, the *Manduca sexta* Hawkmoth. The discussion below considers applications in birds as well as flying insects.

NOMENCLATURE

A_p = Transformed piezoelectric cross-sectional area
A_{ss} = Support structure cross-sectional area
E_p = Piezoelectric modulus of elasticity
E_{ss} = Support structure modulus of elasticity
$I_{x'}$ = Moment of inertia about the x'-axis for the structure
L = Length of the structure
M = Bending moment
P_{avg} = Average power available as body oscillation
$\overline{Y}$ = Centroid for the structure
a_{max} = Peak body acceleration
f = Wing beat frequency
$f_{tip\ mass}$ = Natural frequency of uniform beam with tip mass
$f_{uniform}$ = Natural frequency of uniform beam
$k_{uniform}$ = Stiffness of entire structure
m = Body mass
m_{beam} = Mass of the beam
m_{tip} = Mass of the beam's tip mass
n = Piezoelectric width transformation coefficient
t_p = Piezoelectric thickness
t_{ss} = Support structure thickness
w_p = Transformed piezoelectric width
w_{ss} = Support structure width
$\overline{y}_p$ = Distance from center of piezoelectric to x-axis
$\overline{y}_{ss}$ = Distance from center of support structure to x-axis
σ_p = Piezoelectric maximum bending stress
σ_{ss} = Support structure maximum bending stress
ρ = Radius of curvature

THE WEIGHT CHALLENGE

Wildlife tags allow researchers to study animals in their natural environment, and ideally the sensors have minimal impact on the animal's behavior. Experiments which specifically examine response to mechanical loading are an obvious exception, and these cases are in the minority. The goal therefore is to design tags that minimize the disturbance to the animal, and the two parameters that most affect this are weight and harness design. Harness design often becomes an iterative process, as it can be species-specific. The weight of the tag, usually expressed as a fraction of the animal's body mass, is also in practice species-specific, though general bounds can be set. Cochran [4] suggested the widely cited heuristic that limits tag loading to five percent of animal body mass. However, some migrants cannot tolerate even this modest loading. Pennycuick [5] estimated that transmitters may reduce maximum flight range by 15-34%, an unacceptable amount for birds which may fly non-stop for thousands of kilometers. In practice, the upper limit on loading is generally 2.5-5% of body mass, with emphasis placed on designing for the lower end of this range in order to minimize impacts. This linear heuristic based on body mass is actually a rough approximation, as Marden [6] observed that the maximum lift capacity of a broad range of flying vertebrates and invertebrates is nearly linearly related to the mass of flight muscle, rather than body mass. As the ratio of flight muscle to body mass varies widely across species, so must the acceptable loading ratio. Marden also noted the roughly 25% improvement in efficiency that flying animals are able to realize by using a "clap and fling" flapping motion, which is most prevalent in insects. There are many small flying insects that may tolerate loading ratios an order of magnitude higher than the accepted heuristic for birds.

Though the specific allowable loading ratio clearly varies, a conservative assumption of 2.5% allows generalizations to be made about the applicability of a particular tag. The weight distributions of 6209 species of birds are shown in Figure 1 [7]. The darker shaded bins represent aquatic birds, while the lighter shading represents non-aquatic birds. The x axis shows the weight of the species, scaled by $\log_{10}$.

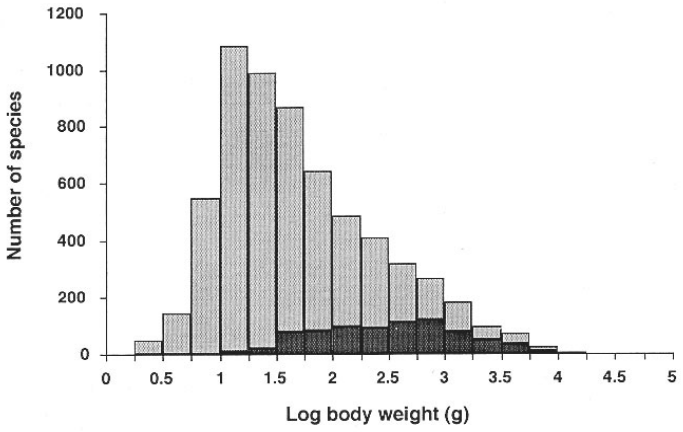

Figure 1. Bird body mass distributions

This plot allows us to make generalizations regarding the applicability of a particular tag. Assume for example that a particular tag weighs 1g. Based on the 2.5% loading heuristic, this tag could be applied to a 40g bird; therefore, only about 60% of bird species would be able to carry this tag. Clearly, reducing tag weight is of critical importance.

Reductions in electronic component sizes have allowed tag manufacturers to incrementally reduce their tag masses. Several manufacturers now sell radio transmitter tags that weigh less than 1 gram, however these devices are universally limited by the amount of energy that can be stored in their batteries. Battery mass consumes as much as 75% of the total weight budget, yet they yield limiting run times. Most animals exhibit behavior with annual periodicity. Many migrants travel thousands of kilometers each year, making field observations difficult or impossible, and a complete accounting of their behavior cannot be obtained with tags that only last for several weeks. Table 1 shows a representative sample of the state of the art in battery technologies that are applicable to animal tagging applications, sorted by mass specific energy density, E_d. Battery number 1 is too large for inclusion in small tags, but is widely used for larger tags. This cell's significantly higher energy density is due to primarily to the volumetric efficiency inherent in larger tags, though the chemistry contributes as well. Most of these batteries are primary, i.e. non-rechargeable, with the exception of 7, 9, and 10. Cell 7 is remarkable in that it maintains the relatively high energy density of primary cells, yet is rechargeable and low-mass. It is a newer lithium polymer type, and the Mylar encapsulation imposes a much lower weight penalty than the other cell's stainless steel housings. This cell is presently being used in our tag designs.

Careful design of the tag's electronics and software can optimize the power requirements of the tag, which minimizes

Table 1. Representative sample of batteries suitable for small tags

Ref #	Chem.	Capacity (mAh)	E (Joules)	Mass (mg)	E_d (J/mg)
1	Li	1200	15552	9600	1.620
2	Li	30	324	600	0.540
3	Li	25	270	520.5	0.519
4	MnO_2	45	243	500	0.486
5	Li	25	270	659	0.410
6	Li	30	324	800	0.405
7	LiPo	10	130	420	0.309
8	Ag_2O	12.5	70	180	0.387
9	LiMn	5	54	300	0.180
10	LiMn	1.2	13	80	0.162

the energy required over the rated lifetime. If the energy capacity of the battery exceeds the demands of the system, then there is clearly no need for the added complexity and weight of energy harvesting. This may be possible for relatively short deployments, or for simple tags with low-power sensors. However, this is not generally the case, and this is particularly true for tags that use radiofrequency communication devices. Transmitting data wirelessly via RF is an energetically expensive operation for small tags. This situation is not likely to be overcome, as the energy demands of the transmitter are primarily driven by the spreading loss, proportional to the square of the range, that the radio waves undergo in transit, and the need for a minimum power level for detection at the receiver. Table 2 gives an example of power consumption for a typical tag deployment with a one-year lifetime. There are three major tasks that the tag must handle: keeping track of its internal time with a real time clock (RTC), reading sensor data, and sending the sensor data to a receiving station. The tag is designed to accumulate and store the data locally, so it only needs to incur the expense of sending data once. It is assumed that the tag reads its sensor once per minute, each reading generates one byte of data and that each read requires one

Table 2. Energy needs for a typical 1 year tag deployment

Operation	I(uA).	T(sec)	E (Joules)
Timekeeping	3	31.5×10^6	283.5
Read Sensor	200	525.6	0.315
Transmit Data	20,000	420.5	25.23
Total			309

millisecond. The tag's operating voltage is 3 volts, and the RF data rate is 10kbps. This configuration represents a device with minimum functionality, and the energy needs are barely met by the available cells. In fact, if any reasonable de-rating is used, the energy needs cannot be met by a small cell. Additionally, more sophisticated functionality is preferred, which would increase the energy needs of the system. Very low-mass vibration energy harvesting systems could address this problem, enabling multi-year tag lifetimes and more sophisticated functionality.

AVAILABLE ENERGY

Energy harvesting from vibrating structures is a relatively new, but well established field with a growing number of texts devoted to the subject. Roundy [8] reviews multiple vibration harvesting modalities, most of which stem from vibration damping theory. In many cases, the source of the vibration can be treated as infinite, and the proof mass can be assumed to be insignificant, relative to the mass of the structure. This is almost certainly not a valid assumption when harvesting mechanical energy from a flapping animal. It is likely that a vibrating proof mass could have a significant impact on the animal's behavior, and harvesting excessive power from flapping could reduce or eliminate an animal's ability to fly.

Marden [6] defined the term "marginal flight muscle ratio" as the ratio of flight muscle mass to total flying mass, including additional loading, at which an animal could just barely take off. Marden determined this ratio to be approximately .16 across all taxa in his study, which included vertebrate and invertebrate fliers and whose members varied in mass from 19mg to 267g, a remarkably consistent result, considering a mass variation of several orders of magnitude. Individual species in his study had un-laden muscle mass to body mass ratios ranging from just below .16 to above .56. The difference between these two ratios represents the amount of power, scaled by mass, which may be extracted while still allowing the animal to fly. For the weaker flyers, this amount may be extremely small. This line of reasoning naturally ignores the behavioral impacts of loading, and the same rationale which applies to mass loading must also apply to extracting energy via harvesting. There is no published heuristic for allowable energy harvesting, however it is useful to work through a few examples to establish rough guidelines. The House sparrow weighs approximately 33g and has a muscle to body mass ratio (MBMR) of .22, while the *Manduca* genus of Hawkmoth weighs approximately 1.9g and has an MBMR of .33 [6]. Flight muscle in aerobic operation has an approximate maximum output power of about 100W/kg (muscle), and is roughly independent of species [9]. An estimate of excess available power can be made by looking at excess available flight muscle, relative to the .16 ratio, which is an assumed minimum. Therefore the House sparrow can produce roughly 710mW and requires at minimum 528mW to fly while Manduca can produce roughly 62mW, and requires at minimum 30mW to fly. These are relatively large numbers when compared with the power requirements of small tags, suggesting that useful energy can be obtained by scavenging a tiny fraction of this amount. The impact of harvesting this energy is unknown, though there is evidence that the impacts on behavior might not be all that severe. Human users of an energy harvesting backpack, which used a sliding mechanism to allow the load to bounce with each stride, experienced less fatigue than expected, based on the energy harvested and the efficiency of muscle. These results might be due to gait adaptation [10]. The same could prove to be true of applications on flying animals.

While the estimates of total flight muscle power given above are useful for placing a bound on the maximum amount of power available, they say nothing about the actual amount of available power, present as vibration of the body, to which it is assumed the harvester will be affixed. If the body is assumed to undergo simple harmonic oscillation in response to the wing beats, then the relationship between the average power during a wing beat cycle (P_{avg}), the body mass (m), the peak body acceleration (a_{max}) and the wing beat frequency (f) is given by Equation 1.

$$P_{avg} = \frac{m a_{max}^{2}}{8\pi^{2} f} \tag{1}$$

The wing beat frequency in Equation 1 has been measured for a variety of flying animals. Wilmott [11] measured a mean wing-beat frequency while hovering of about 26 Hz in the Hawkmoth with high-speed video. Pennycuick [12] observed birds in the field during free flight and noted a wingbeat frequency of about 9 Hz in the Tree Swallow. Other samples of wingbeat frequencies are available, and indicated that wingbeat frequency spans a range of roughly 2 – 30Hz. This wide variation makes it unlikely that a single, one-size-fits-all design will be appropriate. The narrow bandwidth of existing resonant absorber techniques requires tailoring to a specific operating frequency. Intraspecific variation in frequency is of greater concern, as it would be unwieldy to tune each harvester to each animal. As an example, for the Hawkmoth and Tree Swallow, the reported variability in wingbeat frequency (1 SD) was 3.4% and 16%, respectively. This variation must be accounted for if the harvester is to operate efficiently.

While body mass for a wide variety of flying animals is widely available, we were not able to find any data on either body displacement or body acceleration. Without this information, there is no way to evaluate the actual power available for a harvester. Wilmott [11] used high speed video to make detailed measurements of the *Manduca Sexta*, but he did not report body displacement. We set up an experiment to measure body motion in *Manduca Sexta*, which was similar to Wilmott's, though we did not have access to the same camera that he used. Our camera suffered from poor light sensitivity, which made post-processed measurements extremely difficult.

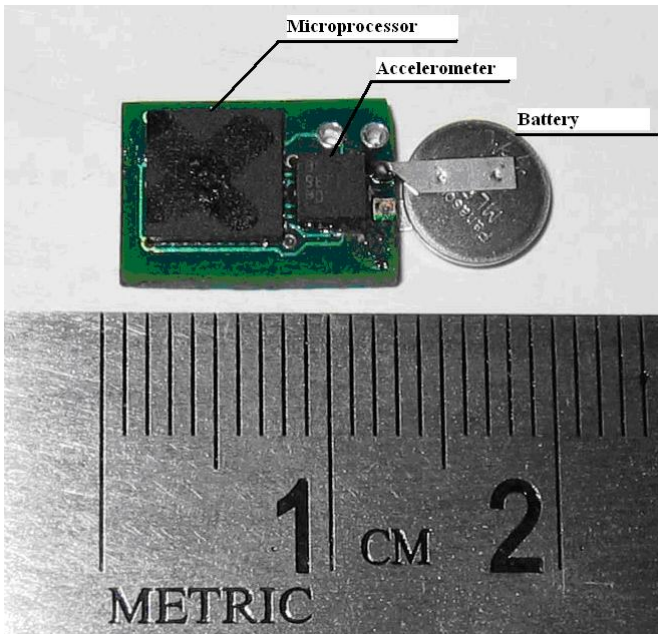

Figure 3. Prototype acceleration logger tag

We decided instead to design an acceleration logger tag to measure the actual acceleration experienced by the body when loaded by a tag. The device, shown in Figure 3, consists of a microcontroller with onboard flash memory, a 3 axis accelerometer, and a battery. The total weight of the system is approximately 860 milligrams. This device records to a 50 second circular buffer at a 200Hz sampling rate. While the mass of the acceleration logger tag will certainly impact the measurements, the goal of this device is to determine the loaded body acceleration, rather then the unloaded acceleration.

We attached the acceleration logger tag to a total of eighteen *Manduca Sexta*, (n=8 male, n=10 female). The acceleration logger was attached via Velcro, making it easily removable. The moths were allowed to fly freely in an enclosure with an interior volume of approximately 4 m^3. For more details of the experimental setup, see [13]. Figure 4 shows a typical mounting arrangement, with the logger attached to the thorax. The Z axis is oriented normal to the acceleration logger circuit board, while the X axis runs forward through the moth's head. The Y axis, following the right hand rule, runs out of the left side of the moth.

A typical time series of the data acquired is shown in Figure 5, while the spectra of a subset of the data from a period of consistent flapping is shown in Figure 6. A similar set of measurements were made on a single Barn Swallow. The dominant flapping frequency and RMS value of acceleration during consistent flapping, for the Hawkmoth and Barn Swallow, are listed in Table 3.

Figure 4. *Manduca Sexta* with acceleration logger attached

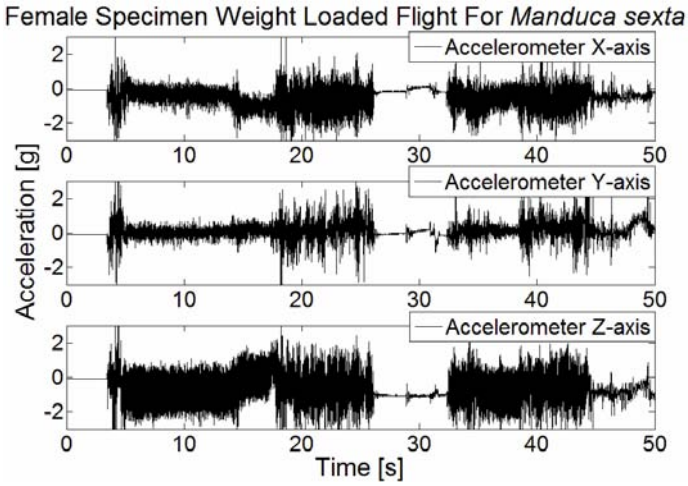

Figure 5. Thorax accelerations of *Manduca Sexta* in flight

The entries from Table 3, when entered into Equation 1, yield an estimate of the actual amount of vibrational power available at the body, the most likely point of attachment. For the Hawkmoth and Barn Swallow, these numbers are 180μW and 38mW, respectively.

Table 3. Flapping frequency and RMS value of body acceleration along Z axis for the Hawkmoth and Barn Swallow during free flight

	f(Hz)	a_Z RMS (g)
Hawkmoth	25	1.2
Barn Swallow	11.5	3.3

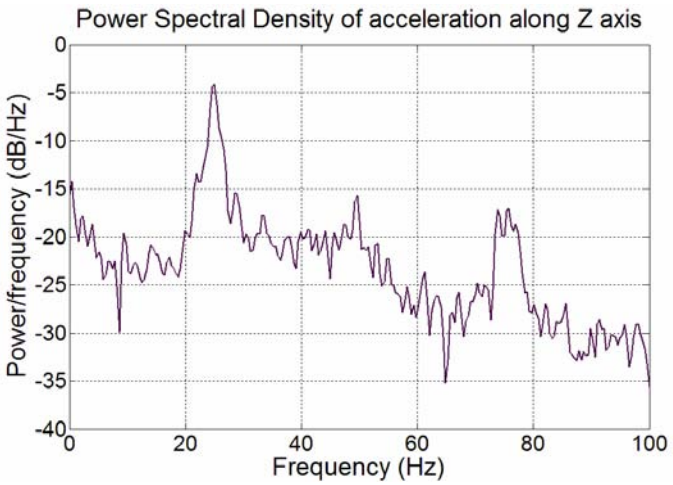

Figure 6. Power Spectral Density of acceleration along Z axis for *Manduca Sexta* in flight

Until this point we have treated the wing-beat frequency as a constant excitation, with a small possible displacement from the mean. Many bird species, including martins and swallows, actually have an irregular flight pattern, with flapping flight interspersed with gliding and erratic turns. A harvester with a high Q beam might never reach the designed strain levels, as the duration of the input signal is too short. Additionally, the phase relationship between the end of one flapping sequence and the beginning of the next is unknown. Were these events to be out of phase, the system performance would suffer, though it seems likely that the bird would adjust the phase of its next wing stroke to match the phase of the harvester's proof mass.

DESIGN APPROACH

The application of piezoelectrics to energy harvesting on flying animals presents several additional challenges, relative to harvesting power from a fixed source of vibration, such as a building or industrial machine. System weight is a primary consideration; after all, the justification for using power harvesting in the first place is to extend tag lifetime without using a large battery. As a practical matter, the present power consumption of microelectronics is such that for all but the most power hungry operations, battery number 1 in Table 1 has sufficient capacity to provide several years of continuous operation in a suitably designed wildlife tag. This sets a rough performance benchmark: if the harvester system is not less than 10 grams, it is of little utility for tag applications,.

The requirement for low mass imposes a host of design challenges, including protecting the piezoelectric element, tuning the resonance of the vibrating structure to match the driving frequency, conditioning the charge output, and storing the harvested energy.

Many power harvesting implementations rely on traditional bulk-crystal beam structures; however these structures are not well suited to wildlife applications. They are fragile, and their stiffness requires either a long structure, or a reasonably large proof mass in order to achieve resonance at the low wing-beat frequencies mentioned earlier. Either of these situations violates the basic requirements of the system. Two other types of piezoelectric materials, PVDF and macro fiber composite (MFC), have mechanical properties more suited to this application. Both materials are quite flexible, and are laminated with tough, waterproof material. We have chosen to ignore PVDF for the time being, since the piezoelectric charge constant of the MFC materials is roughly an order of magnitude larger. MFC materials are a thin, laminate construction, and do not experience significant net strain on their own; they must be bonded to another material in order to achieve a useful magnitude of net charge polarization. The same is true for bulk ceramic structures; hence the familiar uni- and bi-morph construction approach.

Design of a piezoelectric energy harvester typically involves tuning a cantilever beam's resonant frequency to the dominant modal frequency of the host structure. Piezoelectric materials utilize an applied stress with a corresponding induced strain along the beam to generate an electric displacement. This electric displacement of the piezoelectric generates a voltage output. Thus the piezoelectric will act as a transducer of mechanical to electrical energy. Since the piezoelectric generator harnesses physical motion to produce its electrical output, maximum deflection of the structure is desired, within the material's elastic range. At resonance a structure will exhibit this maximum deflection, and the corresponding damping will indicate the bandwidth over which the maximum deflection will span. Piezoelectric energy harvesters primarily assume one of two geometries. The first is a uni-morph device, in which a piezoelectric material is attached on one side of a support structure (Figure 7). The other selection is a bimorph structure which has the piezoelectric attached on either side of the support structure. In selecting which piezoelectric harvester to choose, it is important to first be able to calculate which type can be more readily tuned to the driving frequency of the structure, thus allowing large deflections and corresponding electrical output. In recognizing that the structure in Figure 4 appears as a composite laminate cantilever beam, a static analysis assuming that the first fundamental mode, or first resonance of the structure, is in pure bending will

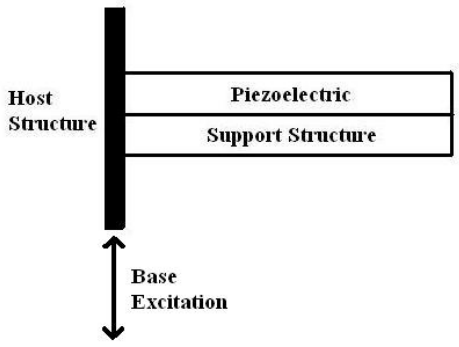

Figure 7. Uni-morph Device

be used for tuning the matching first natural frequency of the structure. This assumption should be acceptable given a relatively thin structure, with a length to width ratio that provides minimal twist, or torsion. This analysis assumes prismatic beams, or constant cross-sectional area along the length of the beam, and also treats the piezoelectric material as homogenous material, a simplification of the material properties. While this simplification does induce an error in the analysis, it can be assumed minor as long as the loading is accepted to be in pure bending and the correct Modulus of Elasticity is implemented along the corresponding axis.

A generic composite beam analysis is thus shown in which the piezoelectric energy harvesters are assumed to be laminate materials under pure bending. To begin, the uni-morph is modeled as shown in Figure 8.

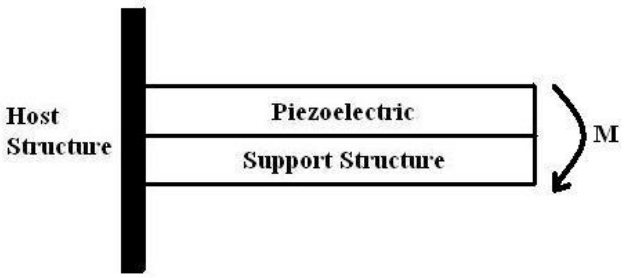

Figure 8. Uni-morph modeled in pure bending

The calculation of the first fundamental frequency f, or natural frequency, of a uniform beam vibrating structure is:

$$f_{uniform} = \frac{\sqrt{k_{uniform} / m_{beam}}}{2\pi} \tag{2}$$

So, given dimensions for each of the laminates, and their corresponding material densities, the entire mass, m, can be found. The entire structure's stiffness, k, however requires more steps in order to be determined. Since the two materials have different material properties, a transformation of the piezoelectric material will be performed in order to represent it as a section of the support structure [14,15]. By taking a ratio of the Modulus of Elasticity of each of the laminates, a coefficient for the transformation of the width of the piezoelectric material can be calculated:

$$n = \frac{E_p}{E_{ss}} \tag{3}$$

This coefficient can then be multiplied by the width of the piezoelectric laminate, parallel to the neutral axis of the entire structure in bending, to create the width of the transformed piezoelectric section.

$$w_p = n w_{ss} \tag{4}$$

With the width of the piezoelectric beam transformed, the entire structure can now be modeled as having the same material properties as that of the support structure. The next item to be calculated is the moment of inertia of the transformed section, but before this can be done, the centroid C, or neutral axis, of the T-shaped cross-section must be calculated (Figure 9).

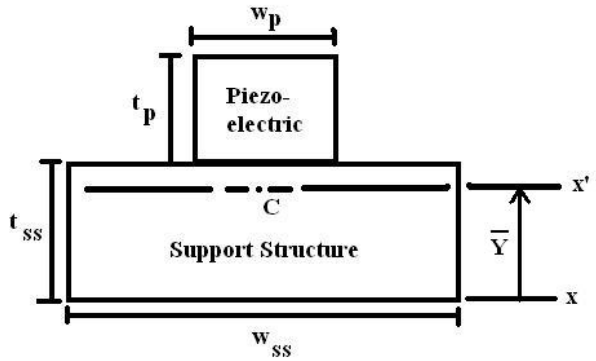

Figure 9. Transformed cross-section

To calculate the centroid of Figure 9, a summation of the areas of the laminates is performed.

$$\sum_{i=p}^{ss} A_i = A_p + A_{ss} = t_p w_p + t_{ss} w_{ss} \tag{5}$$

Next the centers of each of the sections are found from their distances to the x-axis and labeled $\bar{y}_p$ for the piezoelectric layer and $\bar{y}_{ss}$ for the supporting structure. The centers are then multiplied by their corresponding areas and are summed together.

$$\sum_{i=p}^{ss} \left(\bar{y}A\right)_i = \bar{y}_p A_p + \bar{y}_{ss} A_{ss} \tag{6}$$

The centroid can then be found using Equation 7.

$$\bar{Y} = \frac{\sum_{i=p}^{ss} (\bar{y}A)_i}{\sum_{i=p}^{ss} A_i} \tag{7}$$

The centroidal moment of inertia of the entire structure can be found by using the Parallel Axis Theorem. The Parallel Axis

Theorem takes the moment of inertia from each of the areas with respect to the centroid, or x'-axis, and sums them together to obtain the moment of inertia of the entire structure about the x'-axis.

$$I_{x'} = \sum_{i=p}^{ss} (\bar{I} + A\left|\overline{Y} - \overline{y}\right|^2)_i = \sum_{i=p}^{ss} \left(\frac{wt^3}{12} + A\left|\overline{Y} - \overline{y}\right|^2 \right)_i \quad (8)$$
$$= \frac{w_p t_p^3}{12} + w_p t_p \left|\overline{Y} - \overline{y}_p\right|^2 + \frac{w_{ss} t_{ss}^3}{12} + w_{ss} t_{ss} \left|\overline{Y} - \overline{y}_{ss}\right|^2$$

Since the piezoelectric material is a transformed section assumed to have the same material properties as that of the support structure, the stiffness of the entire structure can be found using the following equation which is derived from Euler's formula for a uniform cantilever beam.

$$k_{uniform} = \frac{12.4 E_{ss} I_{x'}}{L^4} \quad (9)$$

Thus an analysis exists in which the natural frequency, near the first resonance motion of the structure, can be calculated in order to maximize the generator performance of the piezoelectric harvester. This analysis can be extended to bimorph configurations by simply adding another piezoelectric laminate to the opposite side of the host structure and summing its transformed section into the analysis.

Other piezoelectric harvesters have been augmented using tip masses to increase the bending moment induced on the system. While adding a tip mass increases the complexity to the analysis presented here, a main concern for the designer is to check the maximum stresses, as well as the radius of curvature, to ensure that the mode of operation remains within the elastic range and recalculate the natural frequency, $f_{tip\ mass}$. To calculate the maximum stress for each of the laminates, the following equations are needed:

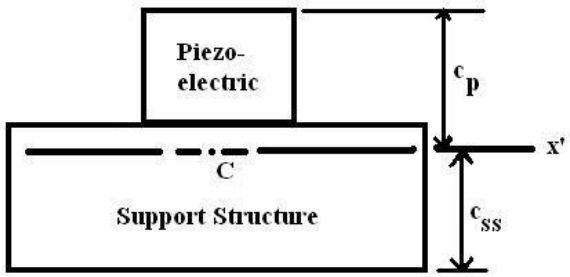

Figure 10. Maximum stress analysis

$$\sigma_p = \frac{Mc_p}{I_{x'}} \quad (10)$$

$$\sigma_{ss} = \frac{Mc_{ss}}{I_{x'}} \quad (11)$$

The maximum stress will indicate if the material will exceed its elastic range under loading. The radius of curvature is also important, as failures have been reported to occur at sharp deflection angles. The following is needed to calculate the radius of curvature for the structure under bending:

$$\rho = \frac{E_{ss} I_{x'}}{M} \quad (12)$$

The natural frequency for the new system, of a cantilever beam with a tip mass added, m_{tip}, is defined using Dunkerley's method [16] for combining solutions for a uniform cantilever beam solution and a mass-less spring with a tip mass, see Equation 13.

$$f_{tip\_mass} = \frac{18.6}{12.4 m_{tip} + 3 m_{beam} L} \left(\frac{E_{ss} I_{x'}}{\pi L^3} \right) \quad (13)$$

Once a suitable mechanical structure for the piezoelectric portion of the harvester has been designed, electronic conditioning circuitry for AC/DC conversion and electrical storage must be added to complete the system. One simple implementation is depicted in Figure 11, which follows the typical path for power harvesters with an AC source. The familiar full wave rectifier is used to obtain a DC voltage, and control circuitry is used to maintain the operating voltage of the piezoelectric near the maximum power transfer point, as described in [17]. On the demonstrator board constructed for this effort, the microcontroller simply turns on a FET to dump current through an LED (series current limiting load resistor not shown). In practice, a DC/DC converter is required to regulate and efficiently step down the output voltage.

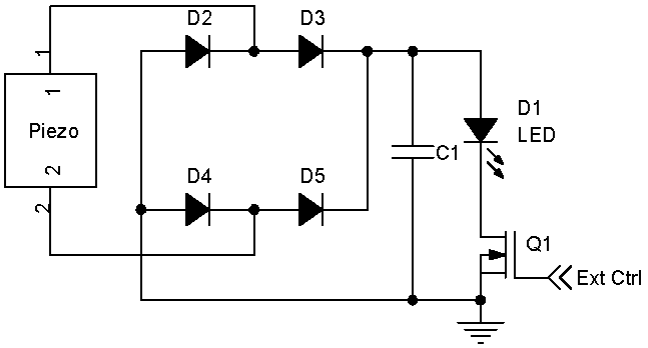

Figure 11. Basic harvesting circuit schematic

Table 4. Components of harvesting schematic

Ref	Description
Piezo	MFC M8503P1 (Smart Material)
D1	67-1878-1 (DigiKey)
D2,D3,D4,D5	BAT54LPDICT (DigiKey)
Q1	DMN5L06WKDICT (DigiKey)
C1	718-1160-1 (DigiKey)

We have implemented a simple harvester circuit, similar to Figure 11, on a small circuit board (comparable in size to the board shown in Figure 3), and plan to soon evaluate the actual power harvested while attached to *Manduca Sexta* and Barn Swallows. This circuit employs low forward voltage drop, ultra low reverse leakage current diodes to minimize power loss in the rectifier. This circuit relies on an ultra-low power micro controller to supervise the power transferred to the load. Note that the microcontroller is not shown in the schematic. The attachment point for the microcontroller is indicated by the "Ext Ctrl" line in the schematic. In practical use as a power supply controller, the light emitting diode shown would be replaced with a buck-converter stage and a larger storage element [17]. This storage element could be either a battery or a suitable capacitor.

DISCUSSION AND CONCLUSION

Wildlife tags are an established means to obtain data from animals in their natural habitat. Developments in microelectronics have expanded the capability and efficiency of these devices, but they are currently limited by power availability. Vibration power harvesters present an appealing avenue for extending the lifetimes of these devices. The application of these techniques presents challenges over and above the challenges of "typical" energy harvesting efforts. We are experimenting with novel piezoelectric materials in an effort to design vibration power harvesters that can tolerate the abuse that they are likely to see "in the field" and that are capable of efficiently harvesting low frequency excitations, while also maintaining very low mass. We have begun to develop systems to measure the actual magnitude and frequency of body oscillations during free flight, and are developing extremely low mass electromechanical systems capable of scavenging, accumulating and consuming harvested energy.

This paper is intended to highlight the critical design parameters, provides the designer a methodology to frequency tune the harvester's cantilever structure using a simplified static composite beam bending analysis, and presents our ongoing development of integrated, ultra-low mass, vibration power harvesting systems.

ACKNOWLEDGMENTS

Partial funding for this research was provided from the DARPA Microsystems Technology Office HiMEMS Program through the Boyce Thompson Institute for Plant Research under the supervision of Dr. Amit Lal.

REFERENCES

[1] Bookhout,T., 1994, "Research and Management Techniques for Wildlife and Habitats," *The Wildlife Society*, Bethesda MD

[2] LeMunyan, C.D., White, W., Nybert, E., 1959, "Design of a Miniature Radio Transmitter for Use in Animal Studies," *Journal of Wildlife Management*, **23**(1), pp. 107-110

[3] Cochran, W.W., Lord, R.D., 1963, "A Radio Tracking System for Wild Animals," *Journal of Wildlife Management*, **27(**1), pp. 9-24

[4] Cochran, W.W., 1972, "Long Distance Tracking of Birds," *Animal orientation and navigation*, **NASA SP-262**, pp. 39-59

[5] Pennycuick, C.J. and Fuller, M.R., 1987, "Considerations of Effects of Radio-Transmitters on Bird Flight," *Biotelemetry*, **IX**, pp. 327-330

[6] Marden, J.H., 1987, "Maximum Lift Production During Takeoff in Flying Animals," *Journal of Experimental Biology*, **130**, pp. 235-258

[7] Gaston, K.J. and Blackburn, T.M., 1995, "The Frequency Distribution of Bird Body Weights: Aquatic and Terrestrial Species," *Ibis*, **137**, pp. 237-240

[8] Roundy, S., Wright, P., and Rabaey, J., 2004, "Energy Scavenging for Wireless Sensor Networks: With Special Focus on Vibrations," *Kluwer Academic*, Boston MA

[9] Ellington, C.P., 1991, "Limitations on Animal Flight Performance," *Journal of Experimental Biology*, **160**, pp. 71-91

[10] Rome, L.C., Flynn, L., Goldman, E.M., and Yoo, T.D., 2005, "Generating Electricity While Walking With Loads," *Science*, **309**, pp. 1725-1728

[11] Wilmott, P., 1997, "The Mechanics of Flight in the Hawkmoth Manduca Sexta" *Journal of Experimental Biology*, **200**, pp. 2705-2722

[12] Pennycuick, C.J., 1990, "Predicting Wingbeat Frequency and Wavelength of Birds" *Journal of Experimental Biology*, **150**, pp. 171-185

[13] Reissman, T., Garcia, E., 2008, "Experimental Study of the Mechanics of Motion of Flapping Insect Flight Under

Weight Loading," *Proceedings of ASME SMASIS Conference*, SMASIS2008, #661

[14] Young, W. C., 1989, "Roark's Formulas for Stress and Strain," *McGraw Hill Publishers*, pp. 117-118

[15] Beer, F. P., and Johnston, E. R., 1992, "Mechanics of Materials," *McGraw Hill Publishers*, pp. 183-207

[16] Dunkerley, S., 1895, "On the Whirling and Vibration of Shafts," Philosophical Transactions of the Royal Society, 185, pp. 269-360

[17] MacCurdy, R.B., Reissman, T., and Garcia, E., 2008, "Energy Management of Multi-Component Power Harvesting Systems", *In Proceedings of SPIE Conference on Smart Materials and Structures*, **6928**, #6928